Metalloporphyrins in Fast Atom Bombardment Mass Spectrometry: Implications for Processes Occurring in the Liquid Matrix

S. Naylor,*,† C. A. Hunter,‡ J. A. Cowan,‡ J. H. Lamb,† and J. K. M. Sanders*,‡

Contribution from the MRC Toxicology Unit, Carshalton, Surrey SM5 4EF, England, and University Chemical Laboratory, Lensfield Road, University of Cambridge, Cambridge CB2 1EW, England. *Received November 27, 1989*

Abstract: The use of fast atom bombardment mass spectrometry is investigated as a technique to study a series of porphyrins (H_2P) and metalloporphyrins (MetP). Rates of demetalation and the redox chemistry of such compounds as well as complex inter- and intramolecular electron-transfer processes are examined. Comparison of the solution chemistry of metalloporphyrins with their behavior in FABMS lead to an understanding of various aspects of the physicochemical events occurring in the FAB matrix. By using FAB matrices with different electronic or acidic properties it is demonstrated that demetalation can occur either by proton displacement or one-electron reduction of the metal. It is also shown that demetalation by protons in FABMS correlates with stability index (S_i) and that the $[H^+]$ in the FAB matrix is $\sim 2 \times 10^{-4}$ M. A model is proposed showing that the gas phase and the selvedge regions of the matrix are in steady-state equilibrium with the liquid matrix. One-electron reductions of $Ag^{II}P$ and $Cu^{II}P$ are shown to occur via an excited-state intermediate, and the rate of electron transfer from the porphyrin ring system to Ag(II) and Cu(II) is calculated to be 2×10^{11} and 7×10^{10} s^{-1}, respectively. The substantially reduced demetalation observed in metalloporphyrin cofacial dimers suggests that the overlap of the metal orbitals of one porphyrin with the proximate π-orbitals of the other porphyrin is weak.

Introduction

The "soft" ionization technique of fast atom bombardment mass spectrometry[1] (FABMS) has been used to analyze a variety of polar, thermally labile compounds.[2] However, FABMS has not been utilized to any great extent for the structure determination of porphyrins and metalloporphyrins. Musselman has investigated hematoporphyrin derivatives[3] and more complex dimeric porphyrins.[4] Other workers have investigated suitable matrices for porphyrins,[5] disproportionation of porphyrins in the FAB matrix,[6] and detection of porphyrin radical cations and anions in FABMS.[7]

The complex series of events that occurs in a liquid matrix containing solute after bombarding with high energy ions or atoms (8–10 keV) and subsequent desorption of secondary ions/molecules into the gas phase is still poorly understood (see refs 8–11 for recent reviews). Numerous models have been proposed,[9,12-16] and, although contentious issues still remain, several common aspects of this complex environment are recognized: (1) The energy of the primary beam (8–10 keV) is converted via a collision cascade into vibrational and ultimately translational energy of secondary ions and molecules. (2) Ion/molecule and electron-transfer reactions occur in the selvedge zone (defined by Rabalais as the plasma formed at and immediately above the matrix surface during sputtering[17]). (3) Unimolecular dissociation of internally excited gas-phase ions/molecules leads to fragmentation.

In particular, the Cooks' model recognizes three different ionization processes which include direct desorption of precharged ions, cationization/anionization/protonation, and electron ionization, which all occur in the selvedge region.[9,12] This work has been expanded on by Kebarle in his gas-phase model. He has presented evidence that numerous collisions of ions and molecules occur in the selvedge region and that gas-phase energetics predominate in the reactions between these high-energy species.[14,15] Work by Van der Peyl[18] suggests that ions desorbed into the gas phase from a liquid matrix possess energies ~0–1.5 eV above their ground state after emerging from the selvedge zone. However, Williams and Naylor[16,20] and Kelner and Markey[19] have presented evidence that these ion energies have a greater range of ~0–3 eV and ~0–5 eV, respectively.

In this paper we present a detailed description of the behavior of porphyrins in FABMS. We have examined both the demetalation reactions and the redox chemistry of metalloporphyrins as well as inter- and intramolecular electron-transfer processes. By comparing the well-documented solution chemistry of metalloporphyrins[21-25] with their behavior in the FAB matrix under

* To whom correspondence should be addressed.
† MRC Toxicology Unit.
‡ University Chemical Laboratory.

(1) Barber, M.; Bordoli, R. S.; Sedgwick, R. D.; Tyler, A. N. *J. Chem. Soc., Chem. Commun.* **1981**, 325.
(2) For a recent review, see: Fenselau, C.; Cotter, R. J. *Chem. Rev.* **1987**, *87*, 501.
(3) Musselman, B. D.; Kessel, D.; Chang, C. K. *Biomed. Environ. Mass Spectrom.* **1988**, *15*, 257.
(4) Musselman, B. D.; Watson, J. T.; Chang, C. K. *Org. Mass Spectrom.* **1986**, *21*, 215.
(5) Meili, J.; Seibl, J. *Org. Mass Spectrom.* **1984**, *19*, 581.
(6) Kurlansik, L.; Williams, T. J.; Campana, J. E. *Biochem. Biophys. Res. Commun.* **1983**, *111*, 478.
(7) Brereton, R. G.; Bazzaz, M. B.; Santikarn, S.; Williams, D. H. *Tetrahedron Lett.* **1983**, *24*, 5775.
(8) Burlingame, A. L.; Baillie, T. A.; Derrick, P. J. *Anal. Chem.* **1986**, *58*, 165R. Burlingame, A. L.; Maltby, D.; Russell, D. H.; Holland, P. T. *Anal. Chem.* **1988**, *60*, 294R.
(9) Pachuta, S. J.; Cooks, R. G. *Chem. Rev.* **1987**, *87*, 647.
(10) Detter, L. D.; Hand, O. W.; Cooks, R. G.; Walton, R. A. *Mass Spectrom. Rev.* **1988**, *7*, 465.
(11) *Desorption Mass Spectrometry. Are SIMS and FAB the Same?*; Lyon, P. A., Ed.; ACS Symposium 1985; p 291.
(12) Pachuta, S. J.; Cooks, R. G. In *Desorption Mass Spectrometry. Are SIMS and FAB the Same?*; Lyon, P. A., Ed.; ACS Symposium, 1985; p 291.
(13) Michl, J. *Int. J. Mass Spectrom. Ion Phys.* **1983**, *53*, 255.
(14) Sunner, J.; Morales, A.; Kebarle, P. *Anal. Chem.* **1988**, *60*, 98.
(15) Sunner, J.; Morales, A.; Kebarle, P. *Int. J. Mass Spectrom. Ion Processes* **1988**, *86*, 169.
(16) Williams, D. H.; Findeis, A. F.; Naylor, S.; Gibson, B. W. *J. Am. Chem. Soc.* **1987**, *109*, 1980.
(17) Honda, F.; Lancaster, G. M.; Fukuda, Y.; Rabalais, J. W. *J. Chem. Phys.* **1978**, *69*, 4931.
(18) Van der Peyl, G. J. Q.; Van der Zande, W. J.; Hoogerbrugge, R.; Kistemaker, P. G. *Int. J. Mass Spectrom. Ion Processes* **1985**, *67*, 147.
(19) Kelner, L.; Markey, S. P. *Int. J. Mass Spectrom. Ion Processes* **1984**, *59*, 157.
(20) Williams, D. H.; Naylor, S. *J. Chem. Soc., Chem. Commun.* **1987**, 1408.
(21) Cowan, J. A.; Sanders, J. K. M. *Tetrahedron Lett.* **1986**, *27*, 1201.
(22) Acid demetalation of $Zn^{II}P$: Shears, B.; Shah, B.; Hambright, P. *J. Am. Chem. Soc.* **1971**, *93*, 776. Acid demetalation of $Mg^{II}P$, see: ref 25.

0002-7863/90/1512-6507$02.50/0

bombardment conditions, aspects of the physicochemical events occurring in FABMS can be rationalized. We present a model for understanding the behavior of porphyrins under FABMS: we show that reactions which occur in the bulk liquid matrix can dominate the appearance of the spectra and, in particular, reactions involving porphyrin excited states often determine the ion pattern observed. This approach has since been used to investigate the properties of some photoactive complex porphyrin assemblies.[26]

Results and Discussion

The positive ion FAB mass spectra of metalloporphyrins are surprisingly complicated. In general, the spectrum of a metalloporphyrin MetP (where P is structure **1**) displays a quasi-molecular ion $(MetPH)^+$, a molecular ion $(MetP)^{\bullet+}$, and two signals due to the corresponding freebase porphyrin $[(H_2PH)^+$ and $(H_2P)^{\bullet+}]$.[27] The dominant signal varies dramatically with the metal, the matrix, and the nature of the substituents and pendant groups on the porphyrin.

The collision cascade in FABMS caused by impacting high energy atoms or ions into the liquid matrix produces protons, electrons, and excited states of analyte molecules. Protonation of basic sites leads to quasi-molecular ions (MH^+, where M in this case refers to MetP). The formation of radical cation molecular ions ($M^{\bullet+}$) is also well documented.[7,16,28] However, in the case of metalloporphyrins a variety of other reactions are also possible. Protons generated in the collision cascade can displace the central metal ion in the porphyrin macrocycle[25] with net substitution or demetalation. This results in the observation of

$$MetP + 2H^+ \rightarrow H_2P + Met^{2+} \quad (1)$$

ion species corresponding to freebase porphyrins and is a further example of substitution reactions that are known to occur in FABMS.[10]

Previous work has demonstrated that an electron-rich medium is created in the matrix. Such electrons can effect metal reductions of the type

$$Cu^{2+} + e^- \rightarrow Cu^+ \quad (2)$$

as described by de Pauw et al.[29] Clearly, uptake of an electron by a metal ion can only occur when the ion has an accessible lower oxidation state. For metalloporphyrins, feasible reactions include Ag(III) → Ag(II) → Ag(I), Cu(II) → Cu(I), Co(III) → Co(II) → Co(I), Mn(III) → Mn(II) → Mn(I), and Fe(III) → Fe(II) → Fe(I). In a lower oxidation state, the metal–porphyrin interaction is generally less stable[25] and so demetalation by protons (eq 1) is facilitated by a one-electron reduction.

The possibility that porphyrin excited states are generated in the selvedge region leads to a variety of considerations. Porphyrins have an electronically excited singlet state 2.0–2.2 eV above their ground state.[23] This state is low enough to be populated assuming that ion energies >1.5 eV are generated in the collision cascade, as suggested by Williams and Naylor[16,20] and Kelner and Markey.[19] When excited, porphyrins become exceedingly good electron donors and readily take part in electron-transfer reactions, hence their use in models for the photosynthetic reaction center.[23,30]

Table I. Correlation between the Extent of Demetalation in Metalloporphyrins and Stability Index (S_i)[25]

MetP (**1**) where metal is	% demetalation[a] in NBA matrix	stability index (S_i)
Mg(II)	92	3.64
Zn(II)	40	4.46
Ag(II)	23	4.60
Co(II)	17	5.78
Cu(II)	4	6.12
Ag(III)	3	8.92[c]
Mn(III)	1	7.15
Co(III)	N/D[b]	9.25

[a] Calculated as ion ratio $[(H_2PH)^+/(MetPH)^+ + (H_2PH)^+] \times 100$. Determined for the average ion abundance of the respective moieties detected after 1–2 min in the fast atom beam. [b] N/D—no loss of metal detected. [c] Calculated from the formula given in ref 25, by using a value of 0.65 Å for the ionic radius of Ag(III) from ref 45.

Table II. Extent of Demetalation for a Series of Monomeric Porphyrins (**1**) as a Function of the FAB Matrix

	% demetalation of monomeric[a] porphyrin (**1**) where metal M is				
matrix	Co(II)	Zn(II)	Mg(II)	Ag(II)	Cu(II)
NBA	17	40	92	23	4
TDG	24	51	95	88	30
AG	N/D[b]	N/D	N/D	N/A[c]	23

[a] As for Table I. [b] N/D—no loss of metal detected. [c] N/A—data not obtained.

Such processes produce porphyrin radical cations and should therefore lead to an enhancement of the intensity of the $M^{\bullet+}$ signal by

$$MetP \rightarrow MetP^* + EA \rightarrow MetP^{\bullet+} + (EA)^{\bullet-} \quad (3)$$

where EA is an electron acceptor.[31]

These electron-transfer reactions also have important implications for demetalation since the electron acceptor can be the metal which is bound in the center of the macrocycle. Electron transfer can thus lead to a one-electron reduction of the metal which in turn facilitates acid demetalation.

The interplay of these mechanisms makes the interpretation of specific metalloporphyrin FAB mass spectra exceedingly difficult. However, by utilizing three different matrices and a series of substituted and capped porphyrins, we have been able to investigate selectively the processes described above. Available FABMS matrices span the pH range, from acidic (thioglycerol) to relatively neutral (glycerol and thiodiglycol, [TDG]) and basic (1-aminoglycerol [AG]). When a basic matrix is used, the concentration of free protons available in the matrix should be dramatically reduced. Thus comparison of the behavior of metalloporphyrins when TDG and AG matrices are used should allow us to establish the role of protons in the matrix reactions. In the presence of an oxidizing matrix such as 3-nitrobenzyl alcohol [NBA], which acts as an electron sink, the concentration of free electrons is reduced, and so the electron reduction processes which occur in other FAB matrices are precluded.[10,16,28] Consequently, comparison of spectra acquired by using TDG and NBA matrices should allow us to determine the significance of one-electron reduction processes.

Demetalation by Protons in the Matrix. The stability of metalloporphyrins in solution with respect to acid demetalation is given by the stability index (S_i). The validity of this theoretical quantity has been confirmed by experiment: the rate or extent of acid demetalation in solution generally correlates with S_i.[25] We have investigated the stability of a series of metalloporphyrins with respect to acid demetalation in the FAB matrix, and our results correlate remarkably well with S_i (Table I). In order to suppress

(23) Harrison, R. J.; Pearce, B.; Beddard, G. S.; Cowan, J. A.; Sanders, J. K. M. *Chem. Phys.* **1987**, *116*, 429.
(24) Hunter, C. A.; Sanders, J. K. M. *J. Am. Chem. Soc.* In press.
(25) Buchler, J. W. In *Porphyrins and Metalloporphyrins*; Smith, K. M., Ed.; Elsevier: 1976; pp 197–199.
(26) Naylor, S.; Cowan, J. A.; Lamb, J. H.; Hunter, C. A.; Sanders, J. K. M. Submitted for publication.
(27) M denotes the molecular ion or the mass of the molecular ion throughout this paper. We have used Met to represent a metal ion to avoid confusion.
(28) Clayton, E. C.; Wakefield, A. J. *J. Chem. Soc., Chem. Commun.* **1984**, 969.
(29) de Pauw, E.; Pelzer, G.; Marien, J.; Natahs, P. In *Ion Formation from Organic Solids*; Benninghoven, A., Ed.; Springer-Verlag: Heidelberg, 1986; Springer Proceedings in Physics, Vol. 9, pp 103–107.
(30) (a) Anderson, H.; Hunter, C. A.; Sanders, J. K. M. *J. Chem. Soc., Chem. Commun.* **1988**, 224. (b) Cowan, J. A.; Sanders, J. K. M.; Beddard, G. S.; Harrison, R. J. *J. Chem. Soc., Chem. Commun.* **1987**, 55.
(31) It is possible that a certain amount of $MetP^{\bullet+}$ is also produced by direct electron ionization with high energy electrons produced in the collision cascade, as noted in the radical cation formation of polyaromatic hydrocarbons in FABMS by Dube, G. *Org. Mass Spectrom.* **1984**, *19*, 242.

the effects of one-electron reductions, we used NBA as the matrix, and to avoid the effects of excited-state electron-transfer reactions, we have considered only the MH^+ signals (although the trends for the $M^{\bullet+}$ signals are in fact similar). Thus demetalation should occur via simple acid proton displacement (eq 1). Table I lists the ratio of ion intensities of the $(H_2PH)^+$ and $(MetPH)^+$ signals averaged over several spectra acquired after 1–2 min in the fast atom beam. The results clearly show agreement between stability of the metalloporphyrin in solution and its behavior in FABMS. A correlation between S_i and rates of demetalation for a series of metalloporphyrins analyzed by electron impact and chemical ionization mass spectrometry has also been made by Beato and Quirke.[32]

Proof that it is actually protons in the matrix which effect these demetalation reactions comes from examining the spectra acquired by using different matrices (Table II). When AG is used, the concentration of protons should be dramatically reduced, thus inhibiting demetalation. However, one-electron reduction processes are also important in this matrix, and so we must consider only metalloporphyrins in which the metal is not readily reduced. Table II shows that $Zn^{II}P$, $Mg^{II}P$, and $Co^{II}P$ are demetalated to similar extents when NBA and TDG matrices are used. This indicates that one-electron reductions do not occur for these species: this is expected for Zn(II) and Mg(II) since they do not have an accessible +1 oxidation state and therefore cannot be reduced by electron-transfer reactions. The Co(II) result is more interesting and will be discussed later. In contrast, $Ag^{II}P$ and $Cu^{II}P$, which do have an accessible +1 oxidation state and are subject to reductive demetalation,[25] show quite different behaviour in NBA and TDG: demetalation increases dramatically in TDG, indicating that one-electron reductions facilitate acid demetalation in this matrix. These reduction reactions will be discussed in detail in the next section.

We will concentrate first on the three species that are demetalated by the simple proton substitution mechanism in eq 1. From Table II, it is clear that matrix protons are responsible for the demetalation process. In AG, where the concentration of freely available protons, generated by the collision cascade, is markedly reduced because of the presence of the basic amino group, little or not demetalation is observed for all three metalloporphyrins even after 10 min in the fast atom beam.

When the FAB mass spectra of $Zn^{II}P$ and $Mg^{II}P$ were studied as a function of time, we observed a steady increase in the intensity of the freebase signal with the length of time for which the sample was exposed to the atom beam. By analogy with our stability index results, this observation suggests that the matrix demetalation reaction proceeds as it would for a metalloporphyrin exposed to small concentrations of acid in solution. Each FAB mass spectrum acquired simply represented a sampling of the course of the reaction at specific time points. The rate equations for acid demetalation of $Zn^{II}P$ and $Mg^{II}P$ in methanol solution have been determined[22] by

$$-\frac{d[MetP]}{dt} = k[MetP]\frac{[H^+]^3}{\rho + [H^+]} \qquad (4)$$

where [MetP] is the concentration of MetP at time t and k and ρ are experimentally determined constants.

If this rate equation is obeyed, then a plot of $\ln\{([MetP]/[H_2P]) + 1\}$ versus time should give a straight line for a constant concentration of protons. The ratio $[MetP]/[H_2P]$ in the matrix at any given time can readily be estimated from the molecular ion abundance of each species observed in the positive ion FAB mass spectrum. We again used NBA as the matrix and considered only the MH^+ signals in order to avoid spurious effects arising from other processes occurring in the matrix. Figure 1 shows the data obtained for $Zn^{II}P$ over a 5-min period. Clearly, the simple rate equation above is followed: the concentration of protons in the FAB matrix is essentially constant, and demetalation occurs in a similar manner to that observed in solution. The same behavior was observed for $Mg^{II}P$, and these results are shown in Figure 2. The proton concentration should depend solely on the nature of the matrix, i.e., $[H^+]$ is constant for the $Mg^{II}P$ and $Zn^{II}P$ experiments, so we can calculate the ratio k_{Mg}/k_{Zn} from the slopes of the plots in Figures 1 and 2.[33] We find that $k_{Mg}/k_{Zn} = 36$, i.e., $Mg^{II}P$ is more rapidly demetalated as is predicted by its lower stability index (Table I). This value compares well with the value of 30 measured for demetalation of Mg(II) and Zn(II) porphyrins in methanol solution.[22]

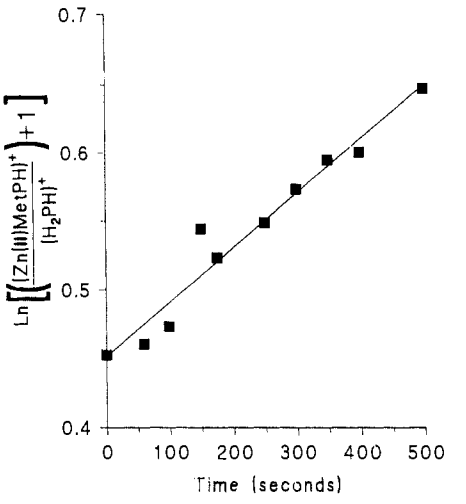

Figure 1. Rate of demetalation for $Zn^{II}MetP$ in positive ion FABMS using NBA as matrix. A plot of $\ln[[(Zn^{II}MetPH)^+/(H_2PH)^+] + 1]$ versus time is presented. The ratio of metalloporphyrin to demetalated species was obtained by determining the ion abundance of m/z = 657 and 595, respectively.

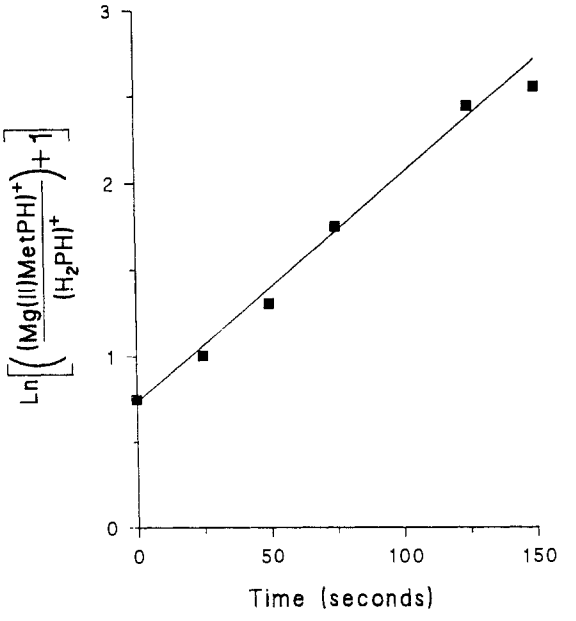

Figure 2. Rate of demetalation for $Mg^{II}MetP$ in positive ion FABMS using NBA as matrix. A plot of $\ln[[(Mg^{II}MetPH)^+/(H_2PH)^+] + 1]$ versus time is presented. The ratio of $MetP/H_2P$ was determined by measuring the ion abundance of m/z = 617 and 595, respectively.

From the above discussion it is clear that *acid demetalation is governed by solution- or liquid-phase kinetics.* Since the values of k and ρ have been experimentally determined in methanol solution for both Mg(II) and Zn(II) porphyrins,[22] it is possible to estimate the concentration of protons in the matrix. From the $Zn^{II}P$ experiment (Figure 1), $[H^+] = 2.4 \times 10^{-4}$ M, and from the

(32) Beato, B. D.; Quike, J. M. E. 35th ASMS Conference on Mass Spectrometry and Allied Topics, Denver, CO, 1987.

(33) We have assumed that the probability for ionization of MetP and H_2P are equal, since unequal ionization rates would change the slopes of plots in Figures 1 and 2 and hence alter k_{Mg}/k_{Zn}.

$Mg^{II}P$ experiment (Figure 2), $[H^+] = 1.7 \times 10^{-4}$ M. This yields an average value of 2×10^{-4} M for the concentration of protons in an NBA matrix. A similar calculation for $Mg^{II}P$ in a TDG matrix gives $[H^+] = 2.4 \times 10^{-4}$ M (results not shown).

The suppression of demetalation when AG is used as a matrix strongly suggests that this process occurs in the matrix itself: it is not the result of decomposition reactions occurring after ionization. However, the question arises as to precisely where and how these reactions occur, particularly in relation to the Kebarle gas-phase model.[15] For $Mg^{II}P$, the freebase signal increases with time and dominates the spectrum after ~1 min in the fast atom beam (Figure 2), and it is difficult to detect a $(MetPH^+)$ ion after 2 min. This suggests that the entire sample has been demetalated.[34] The kinetic experiments show that solution-phase kinetics are followed, i.e., these reactions occur in the bulk liquid phase of the matrix as well as or rather than in the gas-phase or selvedge region. On the basis of the Kebarle model, we suggest that excited, ionized, and protonated species generated in the selvedge zone which do not escape as positively charged ions fall back into the matrix so that an equilibrium is established between the selvedge region and the liquid phase. A result of this equilibrium is that a small but significant concentration of protons (ca. 2×10^{-4} M), free electrons, and excited states is maintained in the bulk liquid matrix. Our results suggest that it is the reactions of these species in the liquid phase which leads to the observed demetalation.[35]

Electron-Transfer Processes. The significance of electron-transfer processes can be established by comparing the behavior of metalloporphyrins in TDG and NBA matrices, as described above. For example, the positive ion FABMS of $Ag^{II}P$ in TDG or tetraglyme as matrix exhibits an abundant freebase porphyrin ion (H_2PH^+) at m/z = 595 $[(Ag^{II}PH)^+/(H_2PH)^+ = 1{:}12]$. However, addition of an electron acceptor, such as benzoquinone, to the matrix reduces demetalation $[(Ag^{II}PH)^+/(H_2PH)^+ = 3{:}1]$. The use of the electron-accepting matrix NBA leads to a dramatic reversal of this signal intensity ratio $[(Ag^{II}PH)^+/(H_2PH)^+ = 24{:}1]$, and, even after 5 min in the xenon beam, the ratio $(Ag^{II}PH)^+/(H_2PH)^+$ is still 12:1. The introduction of an electron sink in the form of the matrix has slowed down the rate of demetalation and implies that electron reduction can be important in the demetalation process.

$$Met^{II}P + e^- \rightarrow Met^{II}P^{\bullet -} \rightarrow [Met^{I}P]^{\bullet -}$$

$$[Met^{I}P]^{\bullet -} + 2H+ \rightarrow H_2P + Met^+ \qquad (5)$$

The metal in the +1 oxidation state is complexed only weakly by the porphyrin, and so acid proton displacement occurs very rapidly. The question of where this electron comes from will be addressed later.

The results in Table II indicate that such reduction processes are important for $Ag^{II}P$ and $Cu^{II}P$. Further evidence for one-electron reduction is obtained when Zn(II) ions are added to the FABMS matrix. In solution, Zn(II) does not displace Ag(II) from a porphyrin.[25] However, in the presence of $Zn(OAc)_2$, the FAB mass spectrum of $Ag^{II}P$ in a TDG matrix shows abundant signals due to $(Zn^{II}P)^{\bullet +}$ and $(Zn^{II}PH)^+$. We rationalize this result on the basis of the pathway below.

$$Ag^{II}P + e^- \rightarrow Ag^{II}P^{\bullet -} \rightarrow [Ag^{I}P]^{\bullet -}$$

$$[Ag^{I}P]^{\bullet -} + Zn^{2+} \rightarrow Zn^{II}P + Met^+ \qquad (6)$$

In contrast to Ag(II), Ag(I) porphyrins are highly unstable,[25] and so the metal is readily displaced by Zn(II) once a reduction reaction has occurred.[36]

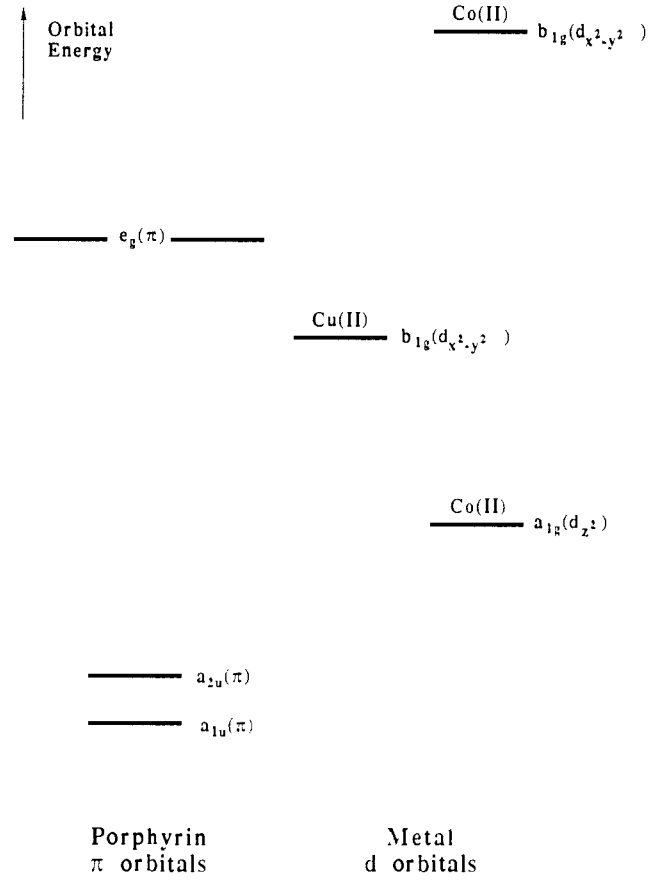

Figure 3. Schematic diagram of the HOMO's and LUMO's of $Cu^{II}MetP$ and $Co^{II}MetP$.

Previous work has shown that $Ag^{II}P$ and $Cu^{II}P$ can be reductively demetalated in solution by reagents such as borohydride.[21] Reduction of the metal center occurs by electron tunneling through the porphyrin π-system, and it has been shown that this process is more efficient for $Ag^{II}P$ than for $Cu^{II}P$.[21] The experiments described below show that reduction occurs via the same mechanism in FAB.

There are three possible mechanisms for reduction of the metal in the porphyrin macrocycle: (1) Mechanism (1) is direct capture of a free electron by the metal.

$$Met^{II}P + e^- \rightarrow [Met^{I}P]^{\bullet -} \qquad (7)$$

(2) Mechanism (2) is capture of a free electron by the porphyrin π-system to give a porphyrin π-radical anion (with electronic configuration $(a_{1u}a_{2u})^2(e_g)^1$ in Figure 3) followed by electron transfer to the metal.

$$Met^{II}P + e^- \rightarrow Met^{II}P^{\bullet -} \rightarrow [Met^{I}P]^{\bullet -} \qquad (8)$$

(3) Mechanism (3) is excitation of the porphyrin to yield an electronically excited state (with electronic configuration $(a_{1u}a_{2u})^1(e_g)^1$ in Figure 3) followed by electron transfer to the metal.

$$Met^{II}P \rightarrow Met^{II}P^* \rightarrow [Met^{I}P^{\bullet +}]^0 \qquad (9)$$
(overall neutral)

Figure 3 shows a schematic diagram of the metalloporphyrin HOMOs and LUMOs. Mechanisms (2) and (3) require delivery

(34) A xenon fast atom at 8 keV produces ~100 protons (80 eV/proton) on impact with the matrix, and a 5 nmol sample of porphyrin requires 10 nmol of protons (~6×10^{15} protons) for complete demetalation to occur. Since a xenon beam flux of 1 μA corresponds to ~10^{14} atoms/s, then complete demetalation requires ~60 s which is consistent with experimental results. We would like to thank a reviewer for bringing this to our attention.

(35) An alternative explanation is provided by the work of Todd, P. J.; Broenewold, G. S. *Anal. Chem.* **1986**, *58*, 895. They present evidence to suggest that desorption from the bulk liquid over time can vary as a function of sample depletion.

(36) A competing pathway of transmetalation can occur via the freebase porphyrin (H_2P).

$$Ag^{II}P \xrightarrow{e^-} Ag^{I}P \rightarrow H_2P \xrightarrow{Zn^{2+}} Zn^{II}P$$

However, using TDG as the matrix, the $[Ag^{II}PH]^+$ ion could still be detected after 5 min in the fast atom beam. Addition of $Zn(OAc)_2$ to an identical sample of $Ag^{II}P$ in TDG resulted in no detectable sign of the $[Ag^{II}PH]^+$ ion during the entire 5 min of bombardment, clearly indicating that in the presence of Zn^{2+} ions loss of Ag is facilitated from the porphyrin.

Table III. Extent of Demetalation of a Series of Substituted Ag(II) Porphyrins

porphyrin	% demetalation[a] in TDG	Rate of electron transfer[b] P → substituent
$Ag^{II}P$ (1)	88	
$Ag^{II}NO_2P$ (2)	45	2×10^{11} s^{-1}
$Ag^{II}BPC$ (3)	69	1×10^{11} s^{-1}

[a] As for Table I. [b] Electron-transfer rate from the porphyrin to the nitro group and pyromellitimide, respectively.

of an electron to the metal via the porphyrin π-system. They involve transfer of an electron from a porphyrin e_g orbital to a metal d orbital (Figure 3), and so we can distinguish them from mechanism (1). We will deal with the difference between mechanisms (2) and (3) in the next section.

We reasoned that if a π-mediated pathway was important then by attaching an electron-withdrawing substituent, such as a nitro group (see **2**), or an electron-accepting cap, such as pyromellitimide (see **3**) to the porphyrin, we should be able to divert electrons away from the metal center and inhibit reductive demetalation. The results are shown in Table III.

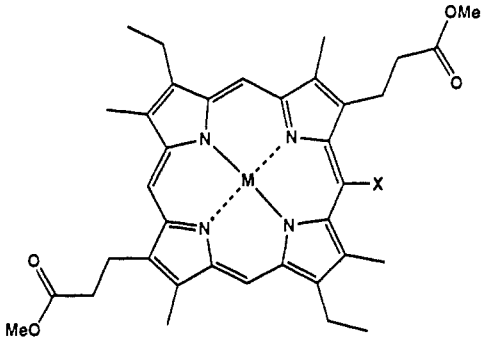

1 X = H
2 X = NO_2

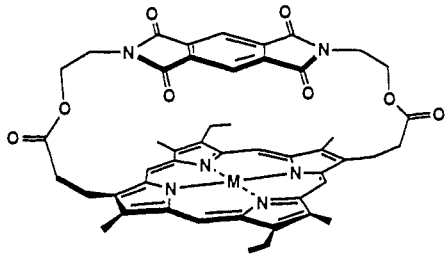

3

With $Ag^{II}NO_2P$ (see **2**), a dramatic decrease in demetalation was observed in TDG, where reductive demetalation is the dominant process (Table III). With $Ag^{II}BPC$ (see **3**), the extent of demetalation was considerably less than for $Ag^{II}P$ but was greater than for $Ag^{II}NO_2P$. NO_2P is a better electron acceptor than P,[37] and so, once the porphyrin π-system picks up an electron, it transfers it much less efficiently to the metal. The nitro group acts as an alternative electron trap. The dramatic inhibition of demetalation by the nitro group shows that electron transfer from the porphyrin π-system to the metal is clearly the dominant process controlling reductive demetalation, and so we can rule out mechanism (1). Similarly, with $Ag^{II}BPC$, the pyromellitimide group acts as an electron sink which siphons off electrons entering the porphyrin π-system preventing reduction of the metal.

The photophysical and redox properties of **2** and **3** in solution have been thoroughly investigated,[23,37] and so the results in Table III can be used as very sensitive probes of the physicochemical behavior of porphyrins in the FAB matrix. The rates of photoinduced electron transfer from the porphyrin to the nitro group of **2** and to the pyromellitimide group of **3** have been measured in CH_2Cl_2 solution by using picosecond spectroscopy (Table III).[23,37] These electron-transfer reactions are very similar to the electron-transfer processes associated with mechanisms (2) and (3) above, since they all involve the transfer of an electron from a porphyrin e_g orbital to an acceptor, a nitro group, a pyromellitimide group, or a metal.

The nitro group inhibits metal reduction dramatically because it traps porphyrin e_g π-electrons very rapidly. The pyromellitimide group performs this function less efficiently because the rate of electron transfer to this acceptor is slower than to the nitro group. There is a striking correlation between the rates of electron transfer in solution and the FABMS results (ignoring the possibility of solvent effects): on going from $Ag^{II}NO_2P$ to $Ag^{II}BPC$, the rate of electron transfer to the acceptor group in solution decreases by a factor of 2, and the extent of demetalation in FABMS increases by a factor of approximately 2. This indicates that reduction of the metal is the result of a simple competition between electron transfer from the porphyrin π-system to the acceptor moiety and electron transfer to the metal. We can therefore use these results to estimate the rate of electron transfer to the Ag(II) center

$$\frac{k_{Met}}{k_{acceptor}} = \frac{[H_2P]}{[MetP]} \qquad (10)$$

where k_{Met} is the rate of electron transfer from the porphyrin to the metal. $k_{acceptor}$ is the rate of electron transfer to the acceptor group,[23] and $[H_2P]$ and [MetP] are estimated, as usual, from their signal intensities in the FAB mass spectrum.

The $Ag^{II}NO_2P$ result gives $k_{Met} = 1.9 \times 10^{11}$ s^{-1} and the $Ag^{II}BPC$ result gives $k_{Met} = 2.2 \times 10^{11}$ s^{-1}, yielding an average value of 2×10^{11} s^{-1}.

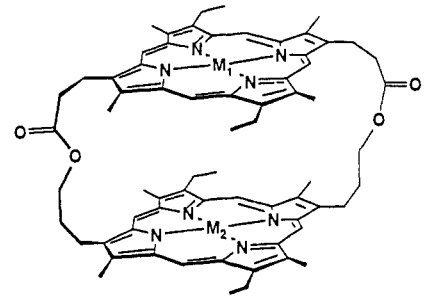

4

This approach opens up new possibilities for the use of FABMS in the investigation of ultrafast electron-transfer processes. Competition experiments of this type allow admittedly crude estimation of rates of reaction on the picosecond time scale. By using a Ag(II) porphyrin, the rate of electron transfer to an acceptor moiety can be gauged by the extent of demetalation. For example, from the extent of demetalation of $Ag^{II}P$ in NBA and by using eq 10, we can estimate the rate of intermolecular electron transfer from the metalloporphyrin to the electron-accepting matrix:

$$k_{et} = \frac{[MetP]}{[H_2P]} \qquad k_{Met} = 3 \times 10^9 \text{ s}^{-1}$$

Reductive demetalation of $Cu^{II}P$ occurs to a lesser extent in the FAB matrix (Table II). This agrees with independent mechanistic work which shows that Ag(II) porphyrins are more amenable to reductive demetalation.[21] Thus the rate of electron transfer from the porphyrin π-system to Cu(II) is considerably slower than to Ag(II). By analogy with the methods above, we estimate a value of ca. 7×10^{10} s^{-1} for electron transfer to Cu(II). We rationalize these results in terms of the Marcus theory in the next section.

The behavior of these systems with time is very similar to that of the porphyrins which were demetalated by the simple acid

(37) Hunter, C. A.; Sanders, J. K. M.; Beddard, G. S.; Evans, S. Unpublished results.

proton displacement mechanism (eq 1); i.e., the intensity of the demetalated signals grows with time and eventually dominate the spectrum, suggesting that demetalation has occurred throughout the matrix. The mixing process required to convert quantitatively solute in the bulk liquid to a different form may include diffusion, but fast atom beam induced "microscopic mixing" may also be involved (see ref 9 for a short review). Whether one-electron reductions can actually occur in the liquid phase is, however, open to debate. Reductive demetalation is a sequential two-step process, and the reduction step may occur exclusively in the high-energy selvedge region.

Excited States. As stated above, excited states are generated in the collision cascade, and, with porphyrins, this can in turn lead to electron-transfer reactions (eq 3, mechanism (3) above). It is possible to determine the relative importance of these excited-state reactions and thus to distinguish between mechanisms (2) and (3) by examining the relative amounts of radical cation ($M^{\bullet+}$) to protonated species (MH^+) in the FAB mass spectrum.

If eq 3 is an important process, it should be associated with an intense radical cation signal. The electron-donating capabilities of different porphyrins (their oxidation potentials) should, therefore, be related to the intensity of the radical cation signal. The ratios $M^{\bullet+}/MH^+$ for both the metalated (MetP) and demetalated (H_2P) signals in the FAB mass spectra of a series of metalloporphyrins are listed in Table IV. The striking feature of these results is that, for almost every entry, the proportion of radical cation is significantly larger in NBA compared to TDG. The electron-accepting matrix clearly stimulates reactions of the type illustrated in eq 3 and so increases the intensity of the radical cation signal. This suggests that electronically excited states are indeed formed in the collision cascade. We now present a detailed analysis of the results in Table IV which provides further evidence to support this hypothesis.

We will consider the $Zn^{II}P$ and $Mg^{II}P$ results first because these systems are not complicated by one-electron reduction processes (see above). In NBA and TDG, the ratio of radical cation to quasi-molecular ion for the freebase signal ($H_2P^{\bullet+}/H_2PH^+$) is essentially constant for H_2P, $Zn^{II}P$, and $Mg^{II}P$. This is further evidence that one-electron reductions do not occur for $Zn^{II}P$ and $Mg^{II}P$ (see later). However, the proportion of radical cation increases dramatically for the metalated signals compared to the freebase signals. The oxidation potential of $Zn^{II}P$ and $Mg^{II}P$ is ca. 0.8 eV as compared with 1.0 eV for H_2P,[23] i.e., the metalated derivatives are better electron donors. Thus the excited-state electron-transfer reactions shown in eq 3 occur more rapidly, and the observed proportion of radical cation increases on metalation.[38]

We now turn to $Ag^{II}P$ and $Cu^{II}P$, where one-electron reduction processes are also important. In the preceding section, we outlined three possible mechanisms for these reactions of which one could be discounted (mechanism (1)). Mechanism (3) involves the formation of a porphyrin excited state prior to metal reduction. If this mechanism is the dominant reductive demetalation pathway, we would expect to see a significant increase in the proportion of radical cation for the demetalated species, compared with the spectrum of the parent freebase porphyrin, H_2P. If mechanism

$$Met^{II}P \rightarrow Met^{II}P^* \rightarrow [Met^{I}P^{\bullet+}]^0$$

$$[Met^{I}P^{\bullet+}]^0 + 2H^+ \rightarrow H_2P^{\bullet+} + Met^+ \qquad (11)$$

(2) dominates no such difference is expected.

$$Met^{II}P + e^- \rightarrow Met^{II}P^{\bullet-} \rightarrow [Met^{I}P]^{\bullet-}$$

$$[Met^{I}P]^{\bullet-} + 2H^+ \rightarrow H_2P + Met^+ \qquad (12)$$

Relative to the parent freebase porphyrin and to the demetalated signals in the $Zn^{II}P$ and $Mg^{II}P$ spectra, Table IV shows that there is a dramatic increase in the $H_2P^{\bullet+}/H_2PH^+$ ratio for the demetalated signals in the spectra of $Ag^{II}P$ and $Cu^{II}P$. This demonstrates unequivocally that mechanism (3) (eqs 9 and 11) is the predominant reductive demetalation pathway.

Thus it is clear that electronically excited states are generated during the bombardment process in FABMS. This is not unreasonable since the lowest porphyrin excited state has an energy

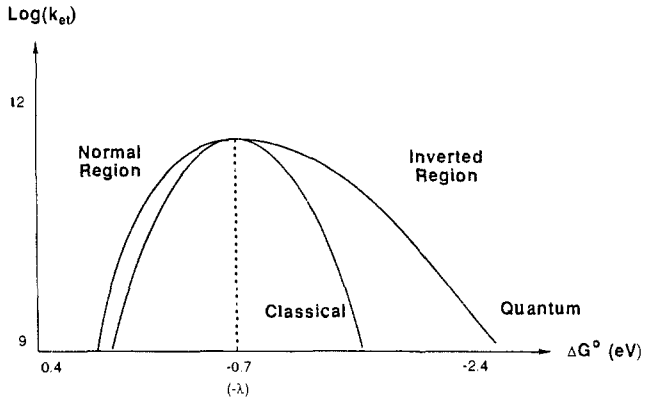

Figure 4. Marcus curve which predicts how the rate of an electron-transfer reaction, k_{et}, depends on $\Delta G°$.

of 2–2.2 eV,[23] well within the 0–3 or 0–5 eV range of energies generated in the fast atom collision cascade in the selvedge region suggested by Williams and Naylor[16,20] or Kelner and Markey,[19] respectively. How such electronic excitation occurs is still under investigation (see Pachuta and Cooks[9] for a review concerning conversion of translational energy into electronic excitation in desorption ionization techniques). We suggest two possible explanations: the large amounts of thermal, translational, and vibrational energy generated in the collision cascade as well as selvedge electron impact may lead to an electronic excitation of the porphyrin π-system; alternatively, the luminescent discharge from ion recombination reactions in the selvedge region may excite the porphyrin π-system.

Having established mechanism (3) as an important pathway in reductive demetalation, we can rationalize why electron transfer to Cu(II) is slower than to Ag(II) and why reduction processes do not occur at all for Co(II) which also has an accessible +1 oxidation state. The rates of electron-transfer reactions can be determined from Marcus theory.[39] In the classical approximation the rate of an electron-transfer reaction, k_{et}, is given by [23,39]

$$k_{et} = \frac{4\pi^2}{h}\frac{1}{(4\pi\lambda kT)^{1/2}}|V(r)^2| \exp\left(-\frac{(\Delta G + \lambda)^2}{4\lambda kT}\right) \qquad (13)$$

where $|V(r)|$ is the orbital overlap integral, λ is the reorganization energy which is found experimentally to be 0.7–1.0 eV,[23] ΔG is the thermodynamic driving force, k is the Boltzmann constant, and T is the temperature.

Figure 4 shows how the rate of electron transfer depends on the driving force, ΔG, and Figure 3 illustrates the orbital energy levels for some first-row transition-metal porphyrin complexes.[40] Metal reduction occurs when an electron is transferred from the porphyrin e_g π-orbital to the lowest unoccupied metal d orbital (the $b_{1g}(d_{x^2-y^2})$ orbital for Ag(II) and Cu(II) or the $a_{1g}(d_{z^2})$ orbital for Co(II)). For example, for Co(II) reduction the reaction in eq 9 may be denoted as

$$(a_{1u}a_{2u})^1(e_g)^1(d_{z^2})^1 \rightarrow (a_{1u}a_{2u})^1(e_g)^0(d_{z^2})^2 \qquad (14)$$

$$(\text{rate} = k_f)$$

However, the back electron transfer from the metal to the porphyrin may also be important ($[Met^{I}P^{\bullet+}]^0 \rightarrow Met^{II}P)^{\bullet}$.

$$(a_{1u}a_{2u})^1(e_g)^0(d_{z^2})^2 \rightarrow (a_{1u}a_{2u})^2(e_g)^0(d_{z^2})^1 \qquad (15)$$

$$(\text{rate} = k_b)$$

(38) This assumes that the rates of these electron-transfer reactions are in the Marcus "normal" region, where k_{et} increases with driving force, ΔG. This is reasonable since, for example, the reduction potential of NBA is ca. −1.1 eV, and so ΔG for electron transfer to this electron-accepting matrix is between −0.1 and 0.3 eV which is clearly in the normal region in Figure 4.

(39) (a) Marcus, R. A. *Faraday Discuss. Chem. Soc.* **1960**, *4*, 21. (b) Marcus, R. A. *Ibid* **1982**, *24*, 7. (c) Marcus, R. A.; Sutin, N. *Biochem. Biophys. Acta* **1985**, *811*, 265.

(40) Zerner, M.; Gouterman, M. *Theor. Chim. Acta* **1966**, *4*, 44.

Table IV. Ratio of Radical Cation to Protonated Ions Detected for a Series of $Met^{II}P$ (**1**) in Positive Ion FABMS by Using Either NBA or TDG as Matrix

	NBA		TDG	
	$(MetP)^{\cdot+}/(MetPH)^+$	$(H_2P)^{\cdot+}/(H_2PH)^+$	$(MetP)^{\cdot+}/(MetPH)^+$	$(H_2P)^{\cdot+}/(H_2PH)^+$
H_2 meso	0.3		0.1	
Zn(II)	1.2	0.2	0.7	0.1
Mg(II)	1.5	0.2	0.9	0.2
Cu(II)	1.1	0.7	0.9	0.7
Ag(II)	1.2	0.8	0.9	0.7

Table V. Extent of Demetalation and One-Electron Reductions Occurring for a Series of Trivalent Porphyrins

monomeric porphyrin (**1**) when metal M is	% demetalation[a]		$(Met^{III}P)^+/(Met^{II}PH)^{+c}$	
	NBA	TDG	NBA	TDG
Mn(III)	1	1	1.8	0.8
Co(III)	N/D[b]	N/D	1.7	0.9
Ag(III)	3	73	1.3	0.6

[a,b] As for Table I. [c] Ratio of the ion abundance of $C^+/(C+1)^+$ after 3 min in the fast atom beam.

Zn(II) and Mg(II) do not have an available empty or half-filled orbital and so cannot be reduced, as we observe experimentally. Assuming that first- and second-row transition metals have a similar orbital energy level distribution, Figure 3 indicates that ΔG for electron transfer from the porphyrin e_g to Ag(II) and Cu(II) should be ca. −0.5 eV.[40] This puts the forward reactions close to the peak of the Marcus curve (Figure 4), i.e., k_f is large and electron-transfer process in eq 14 is fast. ΔG for the back reactions is ca. −1.6 eV,[40] and so k_b (eq 15) is small. Hence a long-lived $[Met^IP^{\cdot+}]^0$ species is generated, and this will be rapidly demetalated by protons in the matrix. In contrast, Figure 3 indicates that, for $Co^{II}P$, the $b_{1g}(d_{x^2-y^2})$ orbital is higher in energy than the porphyrin e_g orbitals, and so the nearest available metal d orbital is very low in energy, $a_{1g}(d_{z^2})$ (Figure 3). Thus ΔG for forward electron transfer from the porphyrin to Co(II) (eq 14) is ca. −1.4 eV,[40] which puts this process in the Marcus "inverted region" where the rates of reaction are slow. ΔG for the back reaction (eq 15) is ca. −0.7 eV (Figure 5),[40] which puts this process close to the peak of the Marcus curve; i.e., the back reaction is very fast. Thus electron reduction of Co(II) will be slow and even if any $[Met^IP^{\cdot+}]^0$ is generated, it will have an exceptionally short lifetime. Consequently we do not observe one-electron reduction for $Co^{II}P$ (Table II).

The difference between Ag(II) and Cu(II) may be explained in terms of the orbital overlap integral, $|V(r)|$. The relatively large, diffuse orbitals of the second-row transition metal, Ag(II), should permit considerably better overlap with the porphyrin π-orbitals than the localized Cu(II) orbitals. This leads to a larger value of $|V(r)|$ for $Ag^{II}P$ and faster electron transfer.

FAB mass spectrometry has been shown to be an excellent tool for investigating ultrafast intramolecular and intermolecular electron-transfer reactions. We have used this approach elsewhere to illustrate how FABMS can be used to examine both the structure and electron-transfer properties of complex multicomponent models for the photosynthetic reaction center.[26]

Trivalent Metalloporphyrins. Trivalent metalloporphyrins differ fundamentally from divalent metalloporphyrins in their behavior under FABMS. Their stability with respect to acid demetalation in NBA does match their relative values of S_i, as discussed above (see Table I). However, trivalent metalloporphyrins are generally associated with a negatively charged counterion, a halide in the systems we have studied. Thus the $[Met^{III}P]^+$ moiety is already positively charged and will be observed as C^+ (C = cation) without the need for further protonation to afford MH^+.

In all three trivalent metals studied, with the exception of $Ag^{III}P$ in TDG,[41] little or no loss of the metal was observed (Table V).

Table VI. Extent of Demetalation for a Series of Bis- and Monometalloporphyrins in NBA and TDG

cofacial metalloporphyrin dimer (**4**) where metals M are	% Demetalation[a]	
	NBA	TDG
$[Ag(II)]_2$	13	39
$[Zn(II)]_2$	N/D[b]	N/D
$[Cu(II)]_2$	N/D	N/D
Cu(II)/Zn(II)	N/D	N/D
$[Co(III)]_2$	N/D	N/D
Zn(II)[c]	18	28
Mn(III)[d]	N/D	N/D

[a] As for Table I. In this case only refers to loss of a single metal ion for the bismetalated porphyrins. [b] N/D—not detected. [c] Metal present in the diol face (M_2 position). [d] Metal present in the acid face (M_1 position).

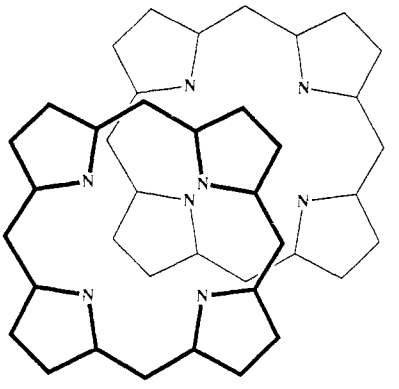

Figure 5. Preferred π-stacking geometry for Zn(II) porphyrins.

However, we observed a signal at $m/z = C + 1$ which increased significantly with time in TDG but not in NBA. This ion corresponds to the protonated species MH^+ and is presumably brought about by a one-electron reduction of the metal, followed by protonation as shown in eq 16.

$$[Met^{III}P]^+ \xrightarrow{e} [Met^{II}P]^0 \xrightarrow{H^+} [Met^{II}PH]^+ \qquad (16)$$

Cofacial Metalloporphyrin Dimers. We have also studied the behavior of a series of cofacial metalloporphyrin dimers in FABMS. Both bis- and monometalated species were investigated. In all cases, demetalation was significantly less than in the corresponding monomers (Table VI). This stabilization of the metalated derivatives in these dimers can again be explained on the basis of porphyrin solution chemistry: it is due to the porphyrin–porphyrin π–π interaction. This phenomenon leads to aggregation in solution and has recently been explained on the basis of a simple electrostatic model of the porphyrin charge distribution.[24] Metalation enhances the porphyrin–porphyrin interaction: the metal center represents a positively charged site at the center of one porphyrin, and so it interacts favorably with the proximate π-electrons of the other porphyrin.[42] The geometry of the stacking interaction is illustrated in Figure 5. Thus the attractive metal–π interaction opposes demetalation of cofacial dimers.

One interesting feature of these results is that, even in cases where one-electron reductions facilitate acid demetalation (Ag(II) and Cu(II)), the metalloporphyrin dimers are more stable with respect to demetalation than the corresponding monomers. We showed above, in such reactions, the electron is delivered from

(41) In the case of $Ag^{III}P$, it appears that the thiodiglycol matrix acts as a competing ligand to remove the metal from the porphyrin. A spectrum acquired after allowing $Ag^{III}P$ to stand for 30 min in TDG showed significantly increased demetalation compared with an identical sample which was analyzed in the spectrometer immediately after addition of the porphyrin to the matrix. A similar experiment was carried out with $Ag^{II}P$, and no evidence for matrix abstraction of the metal was found.

(42) The porphyrin π-system also carries a net negative charge which enhances the π–π interaction further.

the porphyrin π-system to the metal. Furthermore the efficiency of this reaction is governed by the Marcus equation (eq 13), in particular, by the magnitude of the orbital overlap integral, $|V(r)|$. This implies that in these cofacial dimers, although there is a significant electrostatic interaction between the metal and the porphyrin π-system,[24] overlap of the metal orbitals of one porphyrin with the proximate π-orbitals of the other porphyrin is weak. If there were a significant interaction, we would expect demetalation to be increased in the cofacial dimers. These experimental results are in accord with assumptions of our electrostatic model for π–π interactions: except that in some special cases orbital overlap between two π-stacked systems is negligible.[24]

Conclusion

We have shown that metalloporphyrins may be used as subtle probes of the chemistry and physics of processes occurring in the FAB matrix. The behavior of the porphyrins investigated under FABMS mirrors remarkably their behavior in solution with respect to both the kinetics and thermodynamics of acid demetalation, electronic reduction, and electron transfer. We propose a model whereby the gas-phase and selvedge regions of the matrix are in a steady-state equilibrium with the liquid phase. This generates a small ambient concentration of protons (2×10^{-4} M), free electrons, and excited states in the bulk liquid matrix. For porphyrins, reactions of these species apparently dominate the appearance of the spectrum. We have also shown that excited states, probably electronically excited states, are generated in the collision cascade, and this leads to complex electron-transfer processes in the matrix.

By using a series of different matrices, we have shown that it is possible to investigate the complex series of events that occurs in FABMS essentially independently. Our results provide a new insight into the mechanism and kinetics of metalloporphyrin reduction and demonstrate a new approach to the study of ultrafast electron-transfer reactions. Studies of more complex dimeric porphyrins have thrown some light on the nature of the aromatic–aromatic interactions in these systems.[24] These interactions are biologically very important since they are the basis of structure and drug/substrate recognition properties of biomacromolecules such as nucleic acids.[43]

Now that these simple systems have been thoroughly investigated and their behavior explained, FABMS should prove a useful tool for the study of more complex multicomponent assemblies of biomimetic significance.[26]

Experimental Section

Materials and Samples. All solvents used were HPLC grade. The FABMS matrices glycerol, aminoglycerol, thiodiglycol, and 3-nitrobenzyl alcohol were all purchased from Aldrich Chemical Co., U.K. and were vacuum-distilled prior to use. Zinc acetate was purchased from Aldrich and used without further purification.

The syntheses of all porphyrins used in this work have been described previously.[44]

Mass Spectra. All positive ion FAB mass spectra were recorded on one of the following instruments. (1) The first instrument was the Kratos MS50 operating at full accelerating voltage of 8 keV with a mass range of 10 000 daltons. The instrument was equipped with a standard Kratos FAB source and an Ion Tech gun. Xenon was used as the primary atom beam accelerated to 8 keV with an ion current of 1 μA. Spectra were obtained with a magnet scan rate varying between 10 and 100 s per decade, and the data were outputted to a UV chart strip recorder. The source pressure was typically $\sim 1.3 \times 10^{-3}$ Pa (10^{-5} Torr). (2) The second instrument was the VG 70-SEQ of EBQQ geometry operating at full accelerating voltage of 8 keV with a mass range of 3000 daltons. The instrument was equipped with a standard VG FAB source and an Ion Tech gun. Xenon was used as the primary atom beam at 8 keV and 1 μA. Spectra were obtained at a scan rate of 5 s per decade, and the data were collected and processed by using a VG 11/250 system.

Porphyrins were first dissolved in CH_2Cl_2 (which had been passed through a basic alumina column to remove any trace amounts of acid) in order to improve their solubility in the FAB matrix.[26] Typically, ~5 nmol of porphyrin in 2 μL of CH_2Cl_2 was added to 2 μL of matrix on the FAB probe. The sample and matrix were thoroughly mixed and subjected to FAB mass spectrometry. The porphyrin samples in the FAB matrix were subjected to FABMS continuously for ~5 min, and the $(MetPH)^+$ and $(H_2PH)^+$ regions were scanned.

Acknowledgment. We thank the MRC (S.N. and J.H.L.), DENI (C.A.H.), and SERC (J.A.C. and J.K.M.S.) for financial support. J.K.M.S. is a member of the Cambridge Molecular Recognition Centre. We thank one of the reviewers for a number of interesting and valuable comments.

(43) See, for example: Wang, A. H.-J.; Ughetto, G.; Quigley, G.; Rich, A. *Biochemistry* **1987**, *26*, 1152. Burley, S. K.; Petsko, G. A. *Adv. Protein Chem.* **1988**, *39*, 125. Plus references cited therein.

(44) (a) Cowan, J. A.; Sanders, J. K. M. *J. Chem. Soc., Perkin Trans. 1* **1985**, 2435. (b) Cowan, J. A.; Sanders, J. K. M. *J. Chem. Soc., Perkin Trans. 1* **1987**, 2395.

(45) Shannon, R. D.; Prewitt, C. T. *Acta Crystallogr.* **1969**, *B25*, 925.

Comparison of the Calculated Acidity of Cubane with That of Other Strained and Unstrained Hydrocarbons

James P. Ritchie* and Steven M. Bachrach†

Contribution from Los Alamos National Laboratory, Mail Stop B214, Los Alamos, New Mexico 87545. *Received September 5, 1989*

Abstract: Gas-phase acidities of some strained and unstrained hydrocarbons were calculated. The resulting deprotonation enthalpies (DPE's) are within 2–3 kcal mol^{-1} of those observed when extended basis sets are employed, some accounting of the correlation energy is made, and zero-point energy differences are considered. Our best calculated DPE for cubane (406.4 ± 3 kcal mol^{-1}) is significantly greater than that calculated for benzene (397 kcal mol^{-1}) and bicyclobutane (395.4 kcal mol^{-1}), but less than that for cyclopropane (413 kcal mol^{-1}). This result shows that the enhanced kinetic acidity of cubane is reflected in its thermodynamic acidity as well. It is noted that the quantity $\nabla^2\rho_c$(C–H) predicts cubane to be less acidic than cyclopropane, as would correlations against $J_{^{13}C-H}$. Changes of angles between bond paths at carbon upon ionization were calculated. It is found that the change for cubane is unusually large for formal sp^3 centers, thus corroborating the unusual hybridization in the cubyl anion as suggested by Luh and Stock.[1]

Luh and Stock suggested in 1974 on the basis of measured exchange rates that cubane is anomalously acidic.[1] They pointed out that its $J_{^{13}C-H}$ is 155 Hz, while that of cyclopropane is 161 Hz. Well-known hybridization arguments[2] and relationships

† Permanent address: Department of Chemistry, Northern Illinois University, Dekalb, IL 60115.

(1) Luh, T.-Y.; Stock, L. M. *J. Am. Chem. Soc.* **1974**, *96*, 3712–3713.

0002-7863/90/1512-6514$02.50/0